

## Research Article

# Modeling and Control of a Shear-Valve Mode MR Damper for Semiactive Vehicle Suspension

Fanxu Meng  and Jin Zhou 

*College of Mechanical and Electrical Engineering, Nanjing University of Aeronautics and Astronautics, Nanjing 210016, China*

Correspondence should be addressed to Jin Zhou; zhj@nuaa.edu.cn

Received 9 February 2019; Accepted 13 May 2019; Published 30 May 2019

Academic Editor: Nicola Caterino

Copyright © 2019 Fanxu Meng and Jin Zhou. This is an open access article distributed under the Creative Commons Attribution License, which permits unrestricted use, distribution, and reproduction in any medium, provided the original work is properly cited.

Aiming at demonstrating the feasibility and capability of applying magnetorheological (MR) dampers to the vehicle vibration control, the hyperbolic tangent model is established to characterize the performance of a shear-valve mode MR damper that was developed for a vehicle suspension system in this study. An experimentally derived differential evolution (DE) algorithm is used to find the optimal parameters of the model. To demonstrate the effectiveness of the MR damper for semiactive suspension systems, a model was constructed of a quarter-car suspension system with the damper. A fuzzy control algorithm with a correction factor was adopted to control the output force of the damper and obtain better overall control of the performance of the suspension system. Simulation results indicate that the improved fuzzy control algorithm provides a better ride comfort than normal fuzzy control and passive control. Furthermore, the semiactive suspension system displayed effectively vibration suppression thanks to the MR damper combined with corresponding control algorithms.

## 1. Introduction

The suppression of vibration in vehicle suspension systems has recently become an important issue in vehicle dynamics. Passive suspension systems in vehicles do not meet the requirements of ride comfort and driving safety. As a result, more and more attention has been paid to semiactive suspension systems because of their simple structure and low power consumption, while still approximating to the control performance of active suspension. Magnetorheological (MR) dampers are a kind of smart damper, where the working medium uses MR fluid. Unlike traditional hydraulic dampers, the damping characteristics of MR dampers can be quickly and effectively controlled by regulating the current of a magnet coil inside the damper. This makes them well-suited to semiactive suspension control [1–4].

Establishing an accurate mechanical model of MR dampers is an important prerequisite for their application in suspension vibration control. However, the constitutive relation of MR fluids under an external magnetic field is rather complicated, making work in this area especially

challenging. Recently, several MR damper models have been reported, including the Bingham model [5], Bouc-Wen model [6], Improved Dahl model [7], LuGre friction model [8], and ANFIS model [9]. Apart from the ANFIS model, all of these are parametric models. The Bingham model uses only three parameters, so it lends itself well to numerical processing. However, it is too simple to accurately describe the damping force-velocity delay of the MR damper. The other three models offer better accuracy, but they all contain intense nonlinear differential equations, which inevitably results in difficulties in parameter identification. Recently, a mechanical model has been developed that is based on a hyperbolic tangent function, which is employed to describe the hysteretic behavior of MR devices. The use of the explicit mathematical expression was found to improve the accuracy of the model and this has been verified in the literatures [10–12]. As this approach bypasses the need for highly nonlinear equations, it is better at identifying parameters and more suitable for control applications. We therefore draw upon this approach to capture the dynamic characteristics of the MR damper presented in this study. In the case of nonparametric

models, such as the ANFIS model, the identification process is still complicated due to their reliance on special modeling platforms and the long train time.

A semiactive control algorithm is required to precisely control the current or voltage of MR dampers. This makes the application of an advanced control methodology a key aspect of semiactive suspension systems. Numerous control algorithms have been studied in this regard, with the sky-hook control strategy being the most typical, as originally proposed by Karnopp et al. [13]. The essence of this strategy is to provide a simple means of achieving on/ off control, with the current (or voltage) of the MR damper jumping between zero and its maximum value. However, this can lead to self-excited vibration phenomena. Fergani developed an observer-based LPV/ $H_\infty$  controller for MR suspension systems [14]. Simulation results for this controller indicate that it can more effectively reduce the absolute displacement of the sprung mass than would be the case passive suspension. Zhang et al. provided an active disturbance rejection control (ADRC) method to solve the problem of vibration in semiactive suspension systems [15]. However, this kind of control algorithm is relatively complicated and needs the controlled object's model to be extremely accurate. Rashid et al., by contrast, proposed a fuzzy controller for semiactive car suspension systems [16]. This does not rely on a precise mathematical model of the system, and interference from external factors or changes in the system parameters have little impact on the control effect. It also exhibits good levels of robustness. Therefore, it is well-suited to use in automobiles with complicated nonlinear time-variant systems [17–19].

In this paper, a shear-valve mode MR damper is proposed as a way of realizing semiactive control of vehicle suspension systems. In the next section, a description of the damper prototype and an experimental device are presented and the nonlinear characteristics of the damper are investigated experimentally. The hyperbolic tangent model of the MR damper is established in Section 3. In Section 4, an improved fuzzy control algorithm is applied and the performance of a semiactive suspension system with an MR damper is assessed under random road excitation. Finally, the conclusions are presented in Section 5.

## 2. Experimental Testing of the MR Damper

The MR damper employs the magnetic field generated by coil current to change flow behaviors of magnetic packing medium at the gap between the piston and cylinder, so as to carry out the effective control of damping force. According to the operation principle of MR damper, a prototype shear-valve mode MR damper with a double rod structure is first of all manufactured. Figure 1 shows the structure of prototype. The inner cylinder of the device which was filled with commercial MR fluid, MRF-140 (LORD Co., USA), was completely divided into an upper and lower working chamber by the piston. The piston did reciprocating motion in the cylinder. When it moved, the volume of the upper chamber was always equal to volume of the lower chamber. As a result, there is no need for air chamber compensation, thus avoiding the influence of rigid nonlinear compensation

on the damper's properties. The proposed damper was tested using a computer-controlled MTS machine (PA-100, Shenyang, China), which was equipped with force and displacement transducers, as shown in Figure 2. The MTS machine was driven by a hydraulic actuator that could impose an axial load on the specimens. In addition, the MTS machine comprised a powerful signal data acquisition system, which offered complete on-line data acquisition for the damping force and displacement caused by the MR damper. During the experiments, a DC power supply was used to generate current in the EM coil of the MR damper. The excitation signal chosen for the test was a sinusoidal wave with an amplitude of 4 mm. The excitation frequency was set at 2 Hz. The current applied to the magnetic coil was stepped between 0 A and 0.15A at 0.05 A intervals. Additional currents of 0.25A and 0.3A were applied. Hysteretic curves for the measured force-displacement (Figure 3(a)) and force-velocity (Figure 3(b)) were obtained using a 2.0 Hz sine wave signal with a constant amplitude of 4 mm at the different input currents. The results indicate that the hysteretic characteristics of an MR damper strongly depended on the input current.

## 3. Dynamic Modeling of the MR Damper

**3.1. Hyperbolic Tangent Model.** The numerical stability of the hyperbolic tangent model during severe nonlinear damper behavior made it an appropriate choice for characterizing the dynamic response characteristics of MR dampers. The conceptual configuration of the mechanical model is shown in Figure 4. In this model, a hysteretic component is used to describe hysteresis characteristics and a set of spring-dashpot elements is used to describe the viscous damping and stiffness characteristics.

The expression of this model is given as [12]:

$$F(t) = c_0 \dot{x} + k_0 x + \alpha z + f_0 \quad (1)$$

$$z = \tanh(\beta(\dot{x} + \nu \operatorname{sgn}(x))) \quad (2)$$

where  $c_0$  and  $k_0$  are viscous damping and the stiffness coefficients,  $\alpha$  is a scale factor,  $f_0$  is an offset of the output damping force,  $z$  acts as the hysteretic variable,  $\beta$  and  $\nu$  are the shape parameters controlling the slope and width of the hysteresis loops respectively, and  $\operatorname{sgn}(\cdot)$  is the signum function.

Combining these two formulas yields

$$F(t) = c_0 \dot{x} + k_0 x + \alpha \tanh(\beta(\dot{x} + \nu \operatorname{sgn}(x))) + f_0 \quad (3)$$

A set of six constant parameters that relate the characteristic shape parameters to the excitation current was identified and this set of parameters was represented as follows:

$$\Theta = [c_0, k_0, \alpha, \beta, \nu, f_0] \quad (4)$$

**3.2. Estimation Using Sensitivity Analysis.** Sensitivity analysis uses a sensitivity coefficient to show the impact of input variables on the output value of a model [20]. The larger the sensitivity coefficient, the greater the influence of the variable on the output of the model [21–23]. The sensitivity coefficient

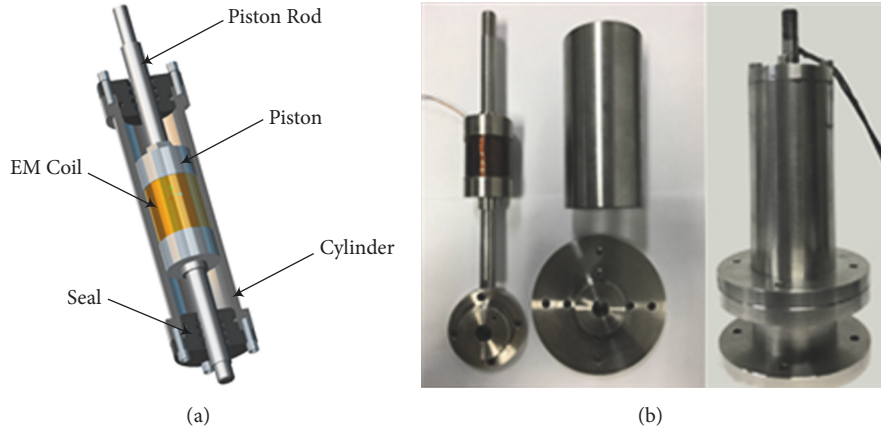


FIGURE 1: Experimental MR damper: (a) schematic; (b) prototype.

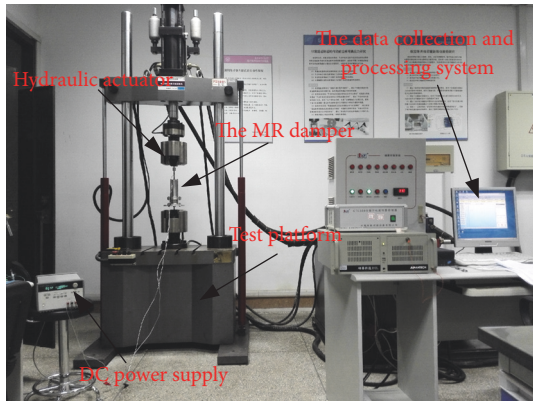


FIGURE 2: Experimental setup.

can be considered as a quantitative expression of parameter sensitivity. Firstly, one model parameter is specified and the output response of hyperbolic tangent model will be solved under the condition that the value of the parameter is gradually changed. Then, the result will be compared with the model output response obtained from the reference value of this parameter to evaluate the influence of the model parameter on the model output. The formula for calculating the sensitivity coefficient is as follows:

$$E = \frac{1}{N} \left[ \sum_{i=1}^N F_i - F'_i \right]^{1/2} \quad (5)$$

where  $F_i$  is the damping force obtained by substituting the reference values of the parameters into the MR damper model;  $F'_i$  refers to the variable parameters substituted into the corresponding damping force obtained by the model.  $N$  is the number of sampling points.

In this study, correlation between the various parameters in the model was not considered. This meant that the other parameters could be fixed while the sensitivity of a single parameter was examined. The reference values of the parameters in the hyperbolic tangent model were defined as

follows:  $\alpha = 110.0233$ ,  $\beta = 0.0774$ ,  $\nu = 7.4899$ ;  $c_0 = 1.6751$ ;  $k_0 = -1.1821$ ;  $f_0 = 1.3044$ . This set of values is obtained by fitting measured responses of the MR damper in which the current is chosen as 0A, and the excitation frequency and amplitude are 2 Hz and 4 mm respectively. The possible variation range of a single parameter in this model was  $\pm 50\%$  of the reference values.

Figure 5 depicts the sensitivity of each parameter in the hyperbolic model. As can be seen, the sensitivity of parameters  $\alpha$  and  $c_0$  is the greatest, with it increasing as the range of variation ranges increases. When  $\beta$  decreases or increases by the same magnitude, the effect of the increment in the value of  $\beta$  upon the model is larger than that of a decrease in the value  $\beta$ . The sensitivity values for the other parameters are less than 0.1, which means they are not sensitive to the output force of the model.

**3.3. Parameter Identification and Validation.** Once a mechanical model is utilized to describe the dynamic characteristics of an MR damper properly, the model's parameters have to be estimated. The differential evolution (DE) algorithm is a novel parallel stochastic optimization method that has attracted lots of attention in recent years [24, 25]. In comparison to other evolutionary algorithms, the DE algorithm has certain disadvantages in terms of optimization and search speed. It uses real number encoding with a difference-based simple mutation operation and a survival strategy of one-to-one competition, thus reducing the complexity of the genetic manipulation. The optimization process of DE algorithm involves three basic operations: mutation, crossover, and selection. Initially, a group of the random initialized population can be generated in the feasible solution space of an optimization problem. Furthermore, through mutation and crossover operations, new individuals would be generated to form new generations. Finally, the selection operation can be performed on the individuals among the two populations to retain the best individuals for the next population. The entire implementation process of the algorithm is performed as described in [26]. In this work, the control parameters used in the DE algorithm are given by the maximum number of

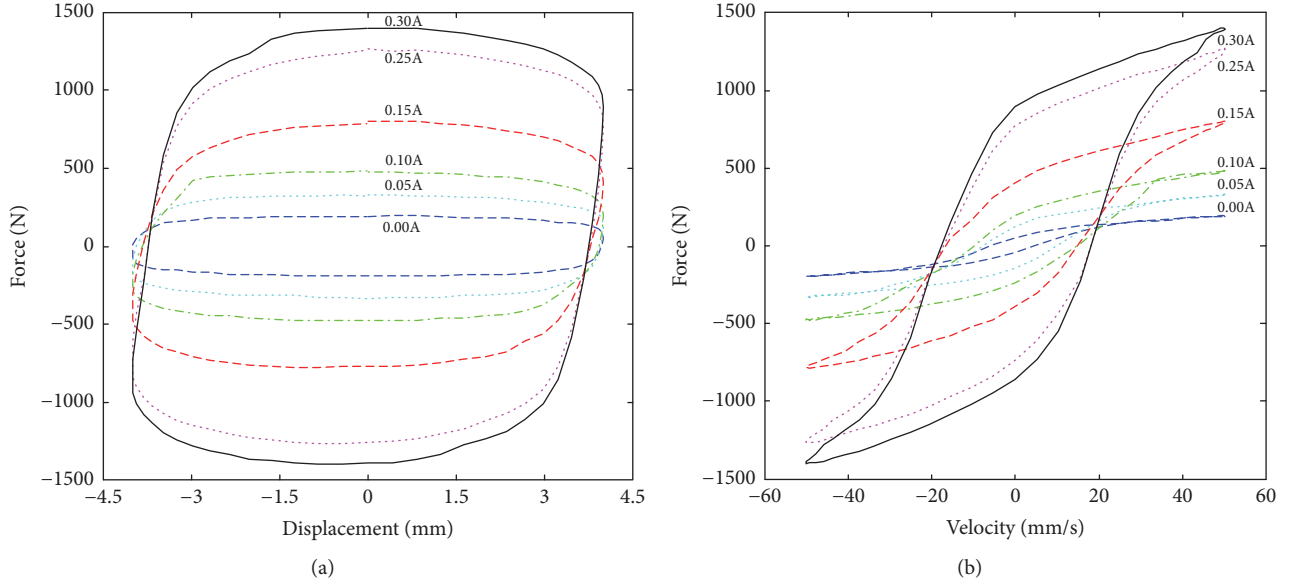


FIGURE 3: Measured hysteretic curves of the MR damper under different currents: (a) force vs. displacement and (b) force vs. velocity.

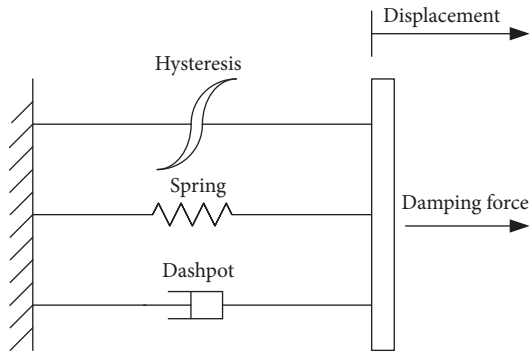


FIGURE 4: Schematic of hyperbolic tangent model.

evolutionary generations  $NP = 400$ , the crossover factor  $CR = 0.8$ , and the mutation scale factor  $F=0.5$ .

Figure 6 depicts a comparison between the measured responses (denoted by the solid line) and estimated responses (denoted by the dotted line) for the experimental MR damper according to different currents. The excitation frequency and amplitude for these tests were 2 Hz and 4 mm. The parameters of the hyperbolic tangent model are represented as a polynomial function relationship of input current  $i$  and are as follows [6, 27, 28]:

$$c_0 = c_{0a}i^2 + c_{0b}i + c_{0c} \quad (6)$$

$$k_0 = k_{0a}i^2 + k_{0b}i + k_{0c} \quad (7)$$

$$\alpha = \alpha_a i^2 + \alpha_b i + \alpha_c \quad (8)$$

$$\nu = \nu_a i^2 + \nu_b i + \nu_c \quad (9)$$

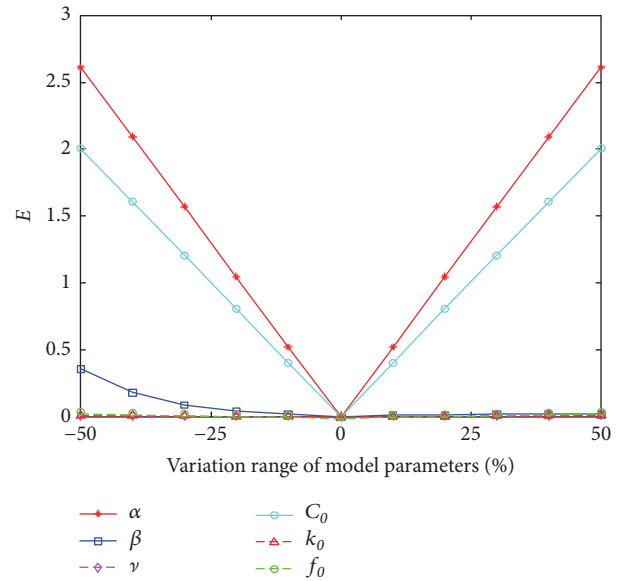


FIGURE 5: Influence of each parameter on the response of hyperbolic tangent model.

The values for the identification parameters of the hyperbolic tangent model at various current levels are listed in Table 1.

## 4. Controller Formulation

**4.1. Quarter-Car Suspension Model with MR Damper.** Prior to executing the semiactive control algorithm, a typical quarter-car model with an MR damper was established (see Figure 7). This model is known to be able to reflect the essential characteristics of a real vehicle suspension system.

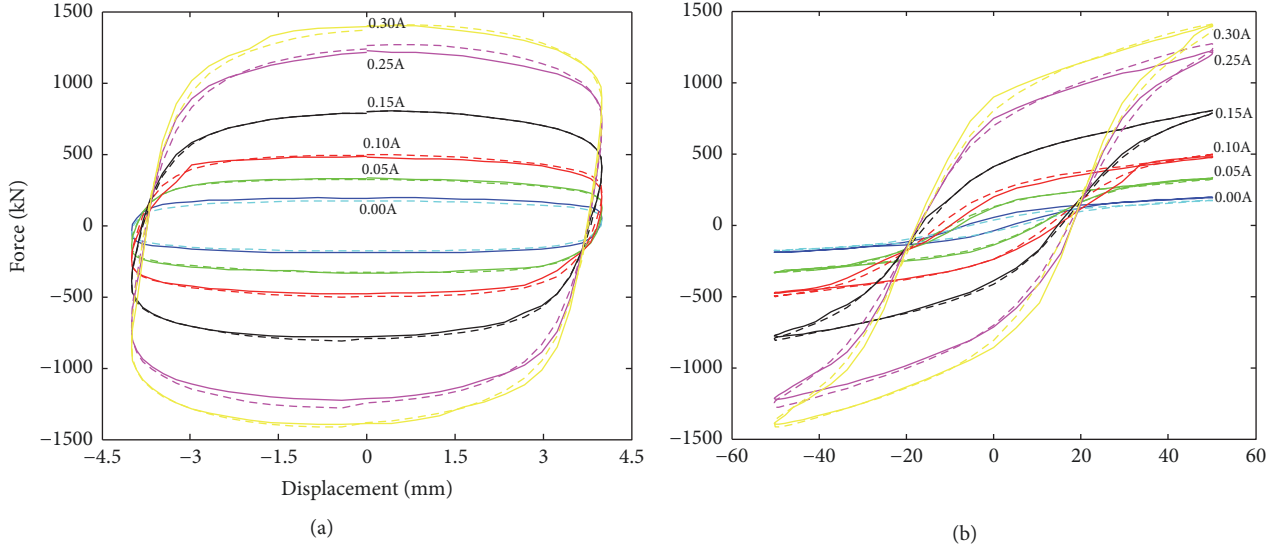


FIGURE 6: Comparison between the estimated and measured responses of the MR damper: (a) force vs. displacement and (b) force vs. velocity.

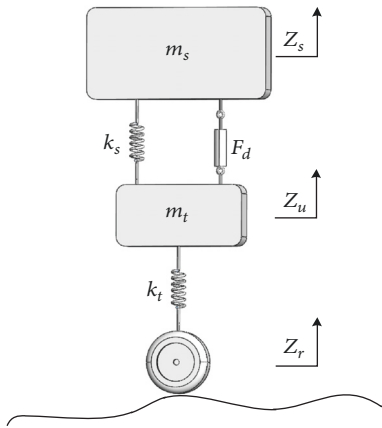


FIGURE 7: Semiactive suspension model.

TABLE 1: Identification results for hyperbolic tangent model using the DE algorithm.

Parameter	Value	Parameter	Value
$c_{0a}$	17 Ns mm <sup>-1</sup>	$\alpha_b$	17.9 N
$c_{0b}$	72 Ns mm <sup>-1</sup>	$\alpha_c$	9.94 N
$c_{0c}$	51 Ns mm <sup>-1</sup>	$\beta$	0.29
$k_{0a}$	6.7 N mm <sup>-1</sup>	$v_a$	31mm s <sup>-1</sup>
$k_{0b}$	-8.54 Ns mm <sup>-1</sup>	$v_b$	56 mm s <sup>-1</sup>
$k_{0c}$	-0.17 Ns mm <sup>-1</sup>	$v_c$	0.96 mm s <sup>-1</sup>
$\alpha_a$	18 N	$f_0$	-0.127 N

By applying Newton's second law, the equations governing the quarter-car model can be expressed as follows:

$$m_s \ddot{z}_s + k_s (z_s - z_u) + F_d = 0 \quad (10)$$

$$m_u \ddot{z}_u + k_t (z_u - z_r) - k_s (z_s - z_u) - F_d = 0 \quad (11)$$

where  $m_s$  is the sprung mass, which represents the car body;  $m_u$  is the unsprung mass, which represents the wheel assembly;  $k_s$  stands for the stiffness of the suspension system;  $k_t$  is the primary stiffness;  $z_s$  is the displacement of the sprung mass;  $z_u$  is the displacement of the unsprung mass;  $z_r$  represents the road excitation;  $F_d$  stands for the controllable force produced by the MR damper. The parameter values for the quarter-car model are determined:  $m_s=391$  kg,  $m_u=50.7$  kg,  $k_s=60000$  N/m, and  $k_t=181000$  N/m.

**4.2. Improved Fuzzy Control.** By using a fuzzy control algorithm with a correction factor, a fuzzy controller can achieve real-time control by changing the correction factor and adjusting the control rules. The principle of the fuzzy control algorithm with a self-set correction factor is shown in Figure 8. The improved algorithm has two key parts: First, it defines a two-dimensional fuzzy system that can take the relative velocity ( $\dot{z}_s - \dot{z}_u$ ) of the suspension and the vertical acceleration ( $\ddot{z}_s$ ) of the car body as its input variables, with the current  $I$  of the MR damper serving as its output variable. The discourse domain of the input variables is set as  $[-1, 1]$ . The corresponding fuzzy language collection is {NB, NS, ZE, PS, PB}, where each element represents negative big (NB); negative small (NS); zero (ZE); positive small (PS); and positive big (PB), respectively. The discourse domain of the output variables is set as  $[-1, 1]$ . The corresponding fuzzy language collection to be taken into account is {S, M, H}. A trigonometric membership function is used for the controller's fuzzy inference. The fuzzy rule table is formed, as illustrated in Table 2. A detailed analysis and description of normal fuzzy control algorithms can be found in [29, 30].

The other part is the correction factor. The correction factor  $K_c$  is determined by established fuzzy rules, as seen in Table 3. The body's vertical acceleration  $\ddot{z}_s$  and the relative velocity of the suspension  $\dot{z}_s - \dot{z}_u$  are taken as the input



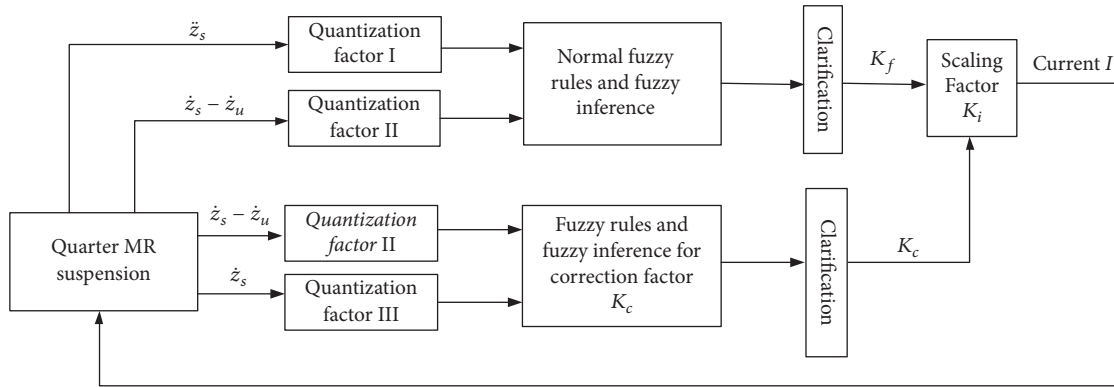


FIGURE 8: Block diagram for fuzzy control algorithm with a correction factor.

TABLE 2: Fuzzy control rules.

$I$	$\dot{z}_s - \dot{z}_u$				
	NB	NS	ZE	PS	PB
NB	S	S	H	H	H
NS	S	S	M	M	M
$\dot{z}_s$ ZE	M	S	S	S	S
PS	M	M	S	S	S
PB	H	H	H	S	L

TABLE 3: Fuzzy rules for correction factor.

$K_c$	$\dot{z}_s - \dot{z}_u$				
	NB	NS	ZE	PS	PB
NB	PB	PM	PS	ZR	ZR
NS	PM	PS	ZR	ZR	ZR
$\dot{z}_s$ ZE	PS	ZR	ZR	ZR	PS
PS	ZE	ZR	ZR	PS	PM
PB	ZE	ZR	PS	PM	PB

TABLE 4: RMS value of the system responses.

Evaluation index	Passive	Fuzzy	Improved fuzzy
Body acceleration/ $m \cdot s^{-2}$	1.0837	0.5458	0.4044
Suspension deflection/m	0.0100	0.0041	0.0036
Tyre displacement/m	0.0042	0.0026	0.0020

language variables. The correction factor is multiplied by the scale factor of the fuzzy controller mentioned above. By changing the value of the correction factor  $K_c$  according to the adjustment of the scale factor, the output force of the MR damper will be changed to enhance the adaptability of the semiactive suspension system to road excitation.

**4.3. Numerical Simulations.** In this section, we report on the numerical simulations of the MR controllable suspension system, as described in Section 4.1. The simulations are carried out using Matlab/Simulink. The MR damper model described in Section 3 is also employed in the simulation. Actual time-domain road displacement input is simulated using the power

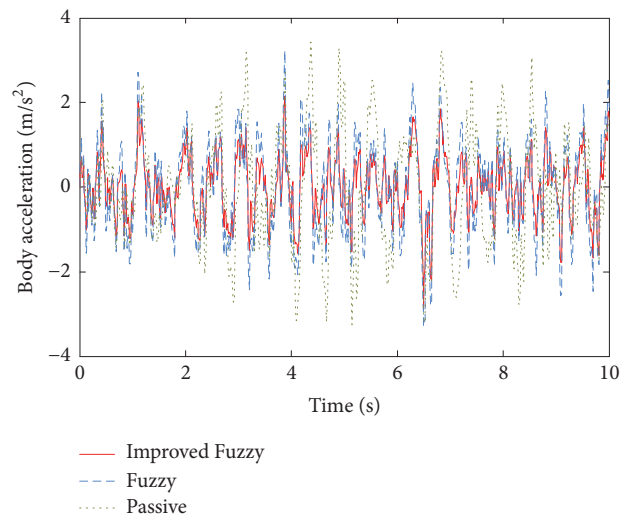


FIGURE 9: Body acceleration response under random road input.

spectrum density of road roughness according to [31], which is defined as

$$\dot{Z}_r(t) = -2\pi f Z_r(t) + 2\pi \sqrt{G_q(n_0)} v \omega(t) \quad (12)$$

where  $Z_r(t)$  is random road excitation input,  $f$  is the cut-off frequency in space domain,  $G_q(n_0)$  is the coefficient of road roughness and set as  $256 \times 10^{-6} m^3$  in the C-level road condition, and  $v$  is the vehicle speed and set as 50 m/s. Analyses of the body acceleration, suspension deflection, and tire displacement under random road input are presented in Figures 9–11 and summarized in Table 4. It is clearly observed that the controlled MR suspension with both the fuzzy controller and the improved fuzzy controller produce a superior damping performance to the passive suspension. For the body acceleration and tire displacement, the improved fuzzy controller generates better results than the ordinary fuzzy controller. It also performed slightly better for the suspension deflection.

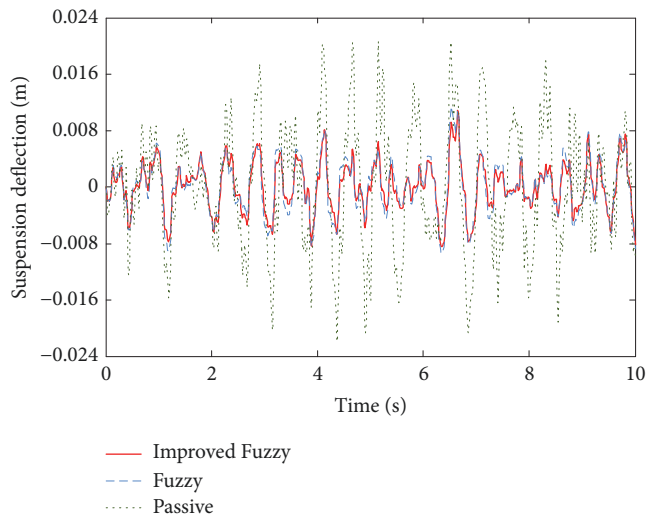


FIGURE 10: Suspension deflection under random road input.

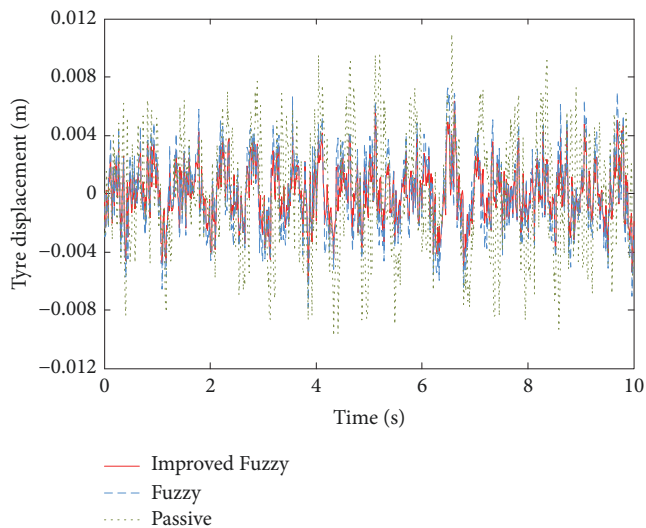


FIGURE 11: Tyre displacement under random road input.

Body acceleration is the primary indicator for evaluating the ride comfort of a vehicle [32]. According to the vibration standard ISO 2631, ride comfort can be evaluated by using the root mean square of the weighed acceleration of a vehicle's body. The RMS value is also calculated for the suspension deflection and tire displacement. As depicted in Table 4, when compared to passive suspension, adoption of fuzzy control with the correction factor and traditional fuzzy control lead to 62.7% and 49.6% reduction in body acceleration, a 64.0% and 59.0% reduction in suspension deflection, and a 54.2% and 38.1% reduction in tire displacement, respectively. Additionally, when compared to traditional fuzzy control, semiactive suspension using fuzzy control with a correction factor produces a better damping effect, indicating that use of the correction factor enhances the adaptability of the controller.

## 5. Conclusions

In this study, a shear-valve mode magnetorheological (MR) damper is developed to improve the vibration suppression in vehicle suspension systems. The hyperbolic tangent model is established to describe the performance of the MR damper based on experimental data generated when the damper was subjected to sinusoidal excitation. Moreover, a sensitivity analysis for each parameter is performed and the influence of the various parameters on the model output is evaluated. The model parameters are identified by the DE algorithm and confirmed as polynomial functions of the current. Finally, a fuzzy control algorithm with a correction factor is applied in simulation to assess the performance of the semiactive suspension system with an MR damper. The simulation results show that the improved fuzzy controller leads to enhance the riding comfort when compared to passive suspension and greater adaptability under random road excitation. In further work, a bench test will be carried out to validate the simulation results for the vibration reduction performance of the proposed MR damper and semiactive control strategy.

## Data Availability

No additional unpublished data are available.

## Conflicts of Interest

The authors declare that they have no conflicts of interest.

## Acknowledgments

This work is supported by the Program of National Natural Science Foundation of China (no. 51675261) and by Funding of Jiangsu Innovation Program for Graduate Education (no. KYLX16\_0324).

## References

- [1] G. Z. Yao, F. F. Yap, G. Chen, W. H. Li, and S. H. Yeo, "MR damper and its application for semi-active control of vehicle suspension system," *Mechatronics*, vol. 12, no. 7, pp. 963–973, 2002.
- [2] Q.-H. Nguyen and S.-B. Choi, "Optimal design of MR shock absorber and application to vehicle suspension," *Smart Materials and Structures*, vol. 18, no. 3, Article ID 035012, 2009.
- [3] R. S. Prabakar, C. Sujatha, and S. Narayanan, "Response of a quarter car model with optimal magnetorheological damper parameters," *Journal of Sound and Vibration*, vol. 332, no. 9, pp. 2191–2206, 2013.
- [4] S. S. Sun, D. H. Ning, J. Yang, H. Du, S. W. Zhang, and W. H. Li, "A seat suspension with a rotary magnetorheological damper for heavy duty vehicles," *Smart Materials and Structures*, vol. 25, no. 10, Article ID 105032, 2016.
- [5] R. Stanway, J. L. Sproston, and N. G. Stevens, "Non-linear modeling of an electro-rheological vibration damper," *Journal of Electrostatics*, vol. 20, no. 2, pp. 167–184, 1987.
- [6] B. F. Spencer Jr., S. J. Dyke, M. K. Sain, and J. D. Carlson, "Phenomenological model for magnetorheological dampers,"

- Journal of Engineering Mechanics*, vol. 123, no. 3, pp. 230–238, 1997.
- [7] N. Aguirre, F. Ikhrouane, J. Rodellar, and R. Christenson, “Parametric identification of the Dahl model for large scale MR damper,” *Structural Control and Health Monitoring*, vol. 19, no. 3, pp. 332–347, 2012.
  - [8] F. Yang, R. Sedaghati, and E. Esmailzadeh, “Development of LuGre friction model for large-scale magneto-rheological fluid dampers,” *Journal of Intelligent Material Systems and Structures*, vol. 20, no. 15, pp. 923–937, 2009.
  - [9] K. C. Schurter and P. N. Roschke, “Fuzzy modeling of a magnetorheological damper using ANFIS,” in *Proceedings of the 9th IEEE International Conference on Fuzzy Systems (FUZZ-IEEE ’00)*, vol. 1, pp. 122–127, IEEE, San Antonio, Tex, USA, 2000.
  - [10] S. Guo, S. Yang, and C. Pan, “Dynamic modeling of magnetorheological damper behaviors,” *Journal of Intelligent Material Systems and Structures*, vol. 17, no. 1, pp. 3–14, 2006.
  - [11] Z. Jiang and R. Christenson, “A comparison of 200 kN magneto-rheological damper models for use in real-time hybrid simulation pretesting,” *Smart Materials and Structures*, vol. 20, no. 6, 2011.
  - [12] N. M. Kwok, Q. P. Ha, T. H. Nguyen, J. Li, and B. Samali, “A novel hysteretic model for magnetorheological fluid damper and parameter identification using particle swarm optimization,” *Sensors and Actuators A: Physical*, vol. 132, no. 2, pp. 441–451, 2006.
  - [13] D. Karnopp, M. J. Crosby, and R. A. Harwood, “Vibration control using semi-active force generators,” *ASME Journal of Engineering for Industry*, vol. 96, no. 2, pp. 619–626, 1974.
  - [14] S. Fergani, L. Menhour, O. Sename, L. Dugard, and B. D’Andrea Novel, “A new LPV/H $\infty$  semi-active suspension control strategy with performance adaptation to roll behavior based on non linear algebraic road profile estimation,” in *Proceedings of the 52nd IEEE Conference on Decision and Control, CDC ’13*, pp. 3511–3516, Florence, Italy, 2013.
  - [15] Z. Zhang, H. R. Karimi, H. Huang, and K. G. Robbersmyr, “Vibration control of a semiactive vehicle suspension system based on extended state observer techniques,” *Journal of Applied Mathematics*, vol. 2014, Article ID 248297, 10 pages, 2014.
  - [16] M. Rashid, M. Hussain, and N. Rahim, “Semi-active car suspension controller design using fuzzy-logic technique,” in *Proceedings of the Conference on Research and Development, SCORED ’02*, pp. 149–152, Shah Alam, Malaysia, 2002.
  - [17] M. M. Rashid, N. A. Rahim, M. A. Hussain, and M. A. Rahman, “Analysis and experimental study of magnetorheological-based damper for semiactive suspension system using fuzzy hybrids,” *IEEE Transactions on Industry Applications*, vol. 47, no. 2, pp. 1051–1059, 2011.
  - [18] A. Shojaei, H. Metered, S. Shojaei, and S. O. Oyadiji, “Theoretical and experimental investigation of magneto-rheological damper based semiactive suspension systems,” *International Journal of Vehicle Structures and Systems*, vol. 5, no. 3-4, pp. 109–120, 2013.
  - [19] S. D. Nguyen, Q. H. Nguyen, and S.-B. Choi, “A hybrid clustering based fuzzy structure for vibration control - Part 2: an application to semi-active vehicle seat-suspension system,” *Mechanical Systems and Signal Processing*, vol. 56-57, pp. 288–301, 2015.
  - [20] R. A. Sharifan, A. Roshan, M. Aflatoni, A. Jahedi, and M. Zolghadr, “Uncertainty and sensitivity analysis of SWMM model in computation of manhole water depth and subcatchment peak flood,” in *Proceedings of the 6th International Conference on Sensitivity Analysis of Model Output, SAMO ’10*, pp. 7739–7740, Italy, July 2010.
  - [21] M. D. Morris, “Factorial sampling plans for preliminary computational experiments,” *Technometrics*, vol. 33, no. 2, pp. 161–174, 1991.
  - [22] I. N. Moggaddam, Z. Salami, and L. Easter, “Sensitivity analysis of an excitation system in order to simplify and validate dynamic model utilizing plant test data,” *IEEE Transactions on Industry Applications*, vol. 51, no. 4, pp. 3435–3441, 2015.
  - [23] D. H. Cho, K. H. Chu, and E. Y. Kim, “A critical assessment of the use of a surface reaction rate equation to correlate biosorption kinetics,” *International Journal of Environmental Science and Technology*, vol. 12, no. 6, pp. 1–10, 2015.
  - [24] R. Storn and K. Price, “Differential evolution. a simple and efficient heuristic scheme for global optimization over continuous spaces,” *Journal of Global Optimization*, vol. 11, no. 4, pp. 341–359, 1997.
  - [25] F. Neri and V. Tirronen, “Recent advances in differential evolution: a survey and experimental analysis,” *Artificial Intelligence Review*, vol. 33, no. 1-2, pp. 61–106, 2010.
  - [26] K. Wang, X. Wang, J. Wang et al., “Solving parameter identification problem of nonlinear systems using differential evolution algorithm,” in *Proceedings of the 2nd International Symposium on Intelligent Information Technology Application, IITA ’08*, pp. 687–691, China, 2008.
  - [27] S. J. Dyke, B. F. Spencer Jr., M. K. Sain, and J. D. Carlson, “Modeling and control of magnetorheological dampers for seismic response reduction,” *Smart Materials and Structures*, vol. 5, no. 5, pp. 565–575, 1996.
  - [28] Y. Yu, Y. Li, J. Li, and X. Gu, “A hysteresis model for dynamic behaviour of magnetorheological elastomer base isolator,” *Smart Materials and Structures*, vol. 25, no. 5, Article ID 055029, 2016.
  - [29] E. H. Mamdani, “Application of fuzzy algorithms for control of simple dynamic plants,” *Proceedings of the IEEE*, vol. 121, no. 12, pp. 1585–1588, 1974.
  - [30] M. Laoufi and A. Eskandarian, “Fuzzy logic control for active suspension of a non-linear full-vehicle model,” in *Proceedings of the IEEE Intelligent Vehicles Symposium*, pp. 677–684, Xi’an, China, 2009.
  - [31] Z. Yonglin and Z. Jiafan, “Numerical simulation of stochastic road process using white noise filtration,” *Mechanical Systems and Signal Processing*, vol. 20, no. 2, pp. 363–372, 2006.
  - [32] I. Karen, N. Kaya, F. Öztürk, I. Korkmaz, M. Yildizhan, and A. Yurttaş, “A design tool to evaluate the vehicle ride comfort characteristics: modeling, physical testing, and analysis,” *The International Journal of Advanced Manufacturing Technology*, vol. 60, no. 5-8, pp. 755–763, 2012.



